

Transient macroscopic quantum superposition states in degenerate parametric oscillation: Calculations in the large-quantum-noise limit using the positive P representation

L. Krippner and W. J. Munro

Department of Physics, University of Waikato, Hamilton, New Zealand

M. D. Reid

Department of Physics, University of Queensland, Queensland 4072, Australia

(Received 26 April 1994)

Recent work by Wolinsky and Carmichael [*OSA Annual Meeting*, 1989 Technical Digest Series Vol. 18, (Optical Society of America, Washington, DC, 1989)] suggests that a superposition of two macroscopically distinct coherent states (a “Schrödinger-cat” state) may be produced in degenerate parametric oscillation in a transient regime. We investigate this possibility by performing numerical simulations of quantum stochastic equations derived using the positive P representation. The equations allow for finite signal cavity loss. Interference fringes which indicate the existence of the macroscopic superposition states are indeed predicted in regimes where the parametric nonlinearity is sufficiently large compared to the signal cavity losses. Experimental criteria needed for the generation of macroscopic quantum superposition states using parametric oscillation are thus established.

PACS number(s): 42.50.Dv

I. INTRODUCTION

The parametric oscillator has played a key role recently in experimental investigations of various quantum properties of the radiation field. Wu *et al.* [1] used degenerate parametric oscillation to obtain a significant reduction in noise (“squeezing”) below the shot-noise level. Heidmann *et al.* [2] obtained a significant squeezing of the radiation field produced from the nondegenerate parametric oscillator operating above threshold. The first experimental realization of the original Einstein-Podolsky-Rosen gedanken experiment was achieved by Ou *et al.* [3] using nondegenerate parametric oscillation. Here measurements of field quadrature phase amplitudes are made to an accuracy of greater than the standard quantum limit. These experimental achievements have been motivated by much theoretical work [4–9].

Most previous theoretical and experimental investigations, however, have focused attention on semiclassical regimes where the effect of quantum noise is to perturb about stable classical solutions. This is the regime relevant to the majority of optical experiments, including the squeezing experiments of Wu *et al.* [1], where the parametric nonlinearities are small. This mode of operation is characterized by very large photon numbers at threshold. The usual theoretical approach in this small-quantum-noise regime is to linearize the quantum fluctuations about the leading classical terms. An exception to this is the nonlinear calculation of Kinsler and Drummond [10]. The degenerate parametric oscillator above threshold displays a bistability. One finds two stable classical field amplitudes differing in phase by 180° . Even in the absence of thermal fluctuations the system may

tunnel from one amplitude to the other because of the presence of quantum noise. Kinsler and Drummond [10] calculate this tunneling time due to quantum noise only. Their calculation, however, still restricts attention to the case of small quantum noise.

There is another mode of operation where the nonlinearity is sufficiently strong that threshold may be reached at very small photon numbers. This is the regime where quantum noise is very large and solutions deviate from a classical description. Previously considered unrealistic such modes of operation may become accessible with the continued development of small-scale devices. Currently, such oscillators might be achievable at microwave frequencies using Josephson nonlinearities [11].

Although the threshold photon number would be very small in these extreme nonlinear quantum oscillators, it is still possible in principle to reach significant intracavity intensities by increasing the input pump power. This raises the question of what new physical properties such macroscopic yet distinctly quantum devices will exhibit and what theories might be used to model them.

Nonlinear steady-state analytical solutions valid for a degenerate parametric oscillator of arbitrary quantum noise strength have been derived by Drummond *et al.* [5] and by Wolinsky and Carmichael [12]. These solutions were obtained in the adiabatic limit where the pump cavity decay rate is much greater than that of the signal. The solutions were obtained using a generalized P -representation expansion of the system density operator. Subsequent work by Carmichael and Wolinsky [13] using the positive P representation indicates that in the absence of all signal loss (this corresponds to the limit of extremely large quantum noise) a signal mode originally in the vacuum will evolve into a quantum superposition of

two coherent states with amplitudes 180° out of phase. For sufficient pump intensities, the intracavity photon number becomes large and the system is predicted to be in a superposition of two macroscopically distinct coherent states. Such states are analogous to those considered by Schrödinger in his famous “Schrödinger-cat” paradox [14], and defy all classical interpretations. Whether or not such cat states exist in the real physical world is not clear. So far there has been no experimental realization, although there have been proposals [15,16]. Quantum mechanics predicts Schrödinger-cat states, but apparently only in the most extreme situations where loss is small.

In the case of the degenerate parametric oscillator, the effect of increasing signal loss is to destroy the superposition effects at least in the steady-state field. In fact it has been shown that the steady-state solutions for arbitrary but finite cavity loss are not coherent state superpositions, but have a classical interpretation [17]. The work of Carmichael and Wolinsky [13], however, is strongly suggestive that Schrödinger-cat states may exist in a transient regime as the signal field evolves from the initial vacuum state.

In order to establish the predicted existence of the Schrödinger-cat states and whether the criteria for the macroscopic quantum superposition states can be met experimentally, one needs to model the transient evolution of the quantum parametric oscillator in regimes of large quantum noise. This is the prime objective of our paper.

The calculations are performed using two methods. The first method involves the careful application of the positive P representation, developed originally by Drummond and Gardiner [18]. The key feature of the representation is the positivity of the distribution function. This enables direct numerical simulation of stochastic equations, which resemble classical equations for field amplitudes except that the dimensions are doubled. Such quantum simulation techniques have been applied successfully to problems involving small quantum noise. The second method is the numerical solution of the master equation using a number state basis. Results using both methods are compared to confirm agreement.

It is important to realize in the positive P -representation case that the stochastic equations used are derived from a master equation with the assumption that certain boundary terms vanish. It is not always the case that these terms do in fact vanish. The problem [19,20] manifests itself most strongly in the large-quantum-noise regime. Work by Smith and Gardiner [20] focused on a system in a large-quantum-noise limit where boundary terms had not been checked. They showed that the results predicted from the incorrect stochastic equations used in this case were wrong. For the case of the parametric oscillator where thermal noise is absent, there is a bounded manifold [12] within which the trajectories starting originally from the origin (an initial condition for the vacuum state) are confined. On this manifold, it can be shown [21] that the relevant boundary terms vanish for arbitrary quantum noise strength. Hence if we restrict attention to the evolution described within this

manifold, we can be sure in this case that the stochastic equations are correct.

II. THE STOCHASTIC EQUATIONS

The interaction Hamiltonian used to model the parametric oscillator is

$$H = \frac{i\hbar}{2} \left(\bar{g} a_2 a_1^{\dagger 2} - \bar{g}^* a_2^{\dagger} a_1^2 \right) + i\hbar\epsilon \left(a_2^{\dagger} - a_2 \right) + \sum_{i=1}^2 a_i^{\dagger} \Gamma_i + a_i \Gamma_i^{\dagger}. \quad (2.1)$$

Here a_i are boson operators for the cavity modes at frequencies ω_i , where $\omega_2 = 2\omega_1$. The mode a_2 is driven by a resonant external driving field with amplitude proportional to ϵ . The loss of photons through the cavity mirrors is modeled by the last term in the Hamiltonian, which denotes a coupling of the cavity modes to the reservoir modes (symbolized by Γ_i) external to the cavity. We will denote the cavity decay rates for modes a_1 and a_2 by γ_1 and γ_2 , respectively.

The stochastic equations we use have been derived previously by Drummond *et al.* [5] and Wolinsky and Carmichael [12]. We summarize the derivation. It is possible to write down the equation for the time evolution of the density operator ρ in the Markovian approximation. One may then expand the density operator in the positive P representation as

$$\rho = \int P(\alpha_i, \alpha_i^{\dagger}) \frac{|\{\alpha_i\}\rangle\langle\{\alpha_i^{\dagger}\}|}{\langle\{\alpha_i^{\dagger}\}|\{\alpha_i\}\rangle} d^2\alpha_1 d^2\alpha_1^{\dagger} d^2\alpha_2 d^2\alpha_2^{\dagger}. \quad (2.2)$$

Here $|\{\alpha_i\}\rangle = |\alpha_1\rangle|\alpha_2\rangle$, where $|\alpha_i\rangle$ is a coherent state and the α_i and α_i^{\dagger} are independent complex variables in phase space. We have the c -number correspondences of $\alpha_i, \alpha_i^{\dagger}$ with a_i, a_i^{\dagger} , respectively. The c -number averages over the positive P distribution are directly related to the normally ordered operator moments. For example,

$$\langle a_1^{\dagger i} a_1^j \rangle = \langle \alpha_1^{\dagger i} \alpha_1^j \rangle. \quad (2.3)$$

An equation of motion for the positive P function may be derived on substitution of (2.2) into the master equation with the assumption that certain boundary conditions are satisfied so that integration by parts is justified. Such a Fokker-Planck equation and an equivalent stochastic differential equation were first derived by Drummond *et al.* [5]. In the limit where the pump mode is much more heavily damped than the signal mode ($\gamma_2 \gg \gamma_1$), it is possible to adiabatically eliminate the pump variables. The final Ito stochastic equations for the signal field are

$$\frac{\partial}{\partial \tau} \begin{bmatrix} x \\ y \end{bmatrix} = \begin{bmatrix} -x + y[\lambda - x^2] \\ -y + x[\lambda - y^2] \end{bmatrix} + \begin{bmatrix} \lambda - g^2 x^2 & 0 \\ 0 & \lambda - g^2 y^2 \end{bmatrix}^{\frac{1}{2}} \begin{bmatrix} \eta(\tau) \\ \eta^{\dagger}(\tau) \end{bmatrix}. \quad (2.4)$$

We have used the scaled variables introduced by Wolinsky and Carmichael [12]. Thus $x = g\alpha_1$, $y = g\alpha_1^\dagger$, $g^2 = \bar{g}^* \bar{g} / 2\gamma_1 \gamma_2$, $\lambda = |\bar{g}\epsilon| / \gamma_1 \gamma_2$, and $\tau = \gamma_1 t$. We consider here the situation where operation of the parametric oscillator is above the semiclassical threshold, corresponding to $\lambda > 1$. In this regime, there are two stable semiclassical solutions $x = y = \sqrt{\lambda - 1}$ and $x = y = -\sqrt{\lambda - 1}$. The $\eta(\tau)$ and $\eta^\dagger(\tau)$ are independent real noise sources with zero mean and satisfying $\langle \eta_i(t) \eta_j(t') \rangle = \delta_{ij} \delta(t - t')$. It was pointed out by Wolinsky and Carmichael [12] that if the initial values of the $\alpha_1, \alpha_1^\dagger$ are real, then the increments $d\alpha_1$ and $d\alpha_1^\dagger$ must also be real. Thus α_1 and α_1^\dagger are restricted to move along the real axes. It is also apparent that the trajectories are confined to move within the bounded manifold $x \leq \sqrt{\lambda}$ and $y \leq \sqrt{\lambda}$.

Equation (2.4) forms the basis of our work here. The situation of interest is where the signal mode is initially in a vacuum state. This initial condition may be represented by $\alpha_1 = \alpha_1^\dagger = 0$. The stochastic equations are converted to Stratonovich form and solved numerically. All trajectories are confined to remain within the bounded manifold. The quantum expectation values at a time t are found by averaging over the results for the different trajectories.

Before performing simulations of the stochastic equations, it is necessary to prove that the boundary terms vanish and thus that the averages calculated from the stochastic solutions correspond to those obtained using the original master equation [21].

III. REVIEW OF ANALYTICAL SOLUTIONS WHICH SUGGEST THE EXISTENCE OF TRANSIENT SCHRÖDINGER-CAT STATES

Steady-state analytical solutions for the density operator in the adiabatic limit $\gamma_2 \gg \gamma_1$ have been obtained by Drummond *et al.* [5] and Wolinsky and Carmichael [12]. By deriving the Fokker-Planck equation equivalent to the stochastic equations one obtains the steady-state solution [12]

$$P_{\text{SS}}(\alpha_1, \alpha_1^\dagger) = [(\lambda - x^2)(\lambda - y^2)]^{1/g^2 - 1} \exp(2xy/g^2). \quad (3.1)$$

The solution is defined over the manifold $|x| \leq \sqrt{\lambda}, |y| \leq \sqrt{\lambda}$. The normally ordered moments $\langle a_1^\dagger{}^n a_1^m \rangle$ are obtained by integration

$$\langle a_1^\dagger{}^n a_1^m \rangle = \int_{\alpha_1^\dagger = -\sqrt{\lambda}}^{\alpha_1^\dagger = \sqrt{\lambda}} \int_{\alpha_1 = -\sqrt{\lambda}}^{\alpha_1 = \sqrt{\lambda}} P_{\text{SS}}(\alpha_1, \alpha_1^\dagger) \times \alpha_1^\dagger{}^n \alpha_1^m d\alpha_1 d\alpha_1^\dagger. \quad (3.2)$$

Carmichael and Wolinsky [13] have pointed out that in the limit of large g , the steady-state distribution approaches a set of δ functions. The corresponding density operator can be expressed as the classical mixture

$$\rho = P_+ |\varphi_+\rangle \langle \varphi_+| + P_- |\varphi_-\rangle \langle \varphi_-|, \quad (3.3)$$

where $|\varphi_\pm\rangle = |\sqrt{\lambda}/g\rangle \pm |-\sqrt{\lambda}/g\rangle$ and

$$P_+ = \frac{1 + \exp[2\lambda/g^2]}{8 \cosh[2\lambda/g^2]}, \quad (3.4)$$

$$P_- = -\frac{1 - \exp[2\lambda/g^2]}{8 \cosh[2\lambda/g^2]}. \quad (3.5)$$

The states $|\varphi_+\rangle$ and $|\varphi_-\rangle$ are quantum coherent state superpositions. For large $\sqrt{\lambda}/g$ the states are superpositions of two macroscopically distinct coherent states. Thus the parametric oscillator operating in the large-quantum-noise and steady-state limits becomes a classical mixture of two Schrödinger-cat states. One of these quantum states $|\varphi_+\rangle$ has an even number of photons. The other $|\varphi_-\rangle$ has an odd number of photons. Carmichael and Wolinsky [13] point out that the state $|\varphi_-\rangle$ is created from $|\varphi_+\rangle$ by loss of a signal cavity photon (and vice versa).

A method for detecting a quantum superposition of two coherent states 180° out of phase has been proposed by Yurke and Stoler [15]. One measures the probability distributions $P(z)$ and $P(p)$ for obtaining results z and p upon measurement of the quadrature phase amplitudes $X_1 = (a_1 + a_1^\dagger)/2$ and $X_2 = (a_1 - a_1^\dagger)/2i$, respectively. If the field is in the coherent state superposition $|\varphi_+\rangle$, the distribution $P(z)$ becomes, for the case where $\sqrt{\lambda}/g$ is large, two Gaussian peaks with centers corresponding approximately to $\sqrt{\lambda}/g$ and $-\sqrt{\lambda}/g$. The distribution $P(p)$ exhibits interference fringes, which are a consequence of the superposition nature of the state $|\varphi_+\rangle$. These fringes are absent in the $P(p)$ for fields which are classical mixtures of $|\sqrt{\lambda}/g\rangle$ and $|-\sqrt{\lambda}/g\rangle$. Calculation of the $P(p)$ for an arbitrary mixture of $|\varphi_+\rangle$ and $|\varphi_-\rangle$ reveals that the fringes are diminished and cancel when the states carry equal weight. These effects are illustrated in Fig. 1. If we examine the prediction (3.3) for the oscillator solution, it is seen that for large $\sqrt{\lambda}/g$, the probabilities P_+ and P_- are comparable and the steady-state field exhibits no signature of quantum interference in its $P(p)$ distribution. As $\sqrt{\lambda}/g$ approaches zero, the P_+ becomes larger than P_- . Although this is suggestive of the formation (at low $\sqrt{\lambda}/g$ values) of $|\varphi_+\rangle$ in the steady state, calculation of the $P(p)$ shows that no fringes will be observed for any finite value of $\sqrt{\lambda}/g$. This has been shown to be true for the steady-state field regardless of the value of g and $\sqrt{\lambda}/g$ [17].

Carmichael and Wolinsky [13] have pointed out, however, that the expansion (3.3) of the steady-state density operator is suggestive of the formation of transient superposition states. The states $|\varphi_+\rangle$ and $|\varphi_-\rangle$ have even and odd photon numbers, respectively. The large g limit for which the expansion is valid corresponds also to the limit of no signal photon cavity loss $\gamma_1 \rightarrow 0$. A model Hamiltonian for the oscillator in the fast-decaying pump limit and in the absence of single-photon cavity loss is

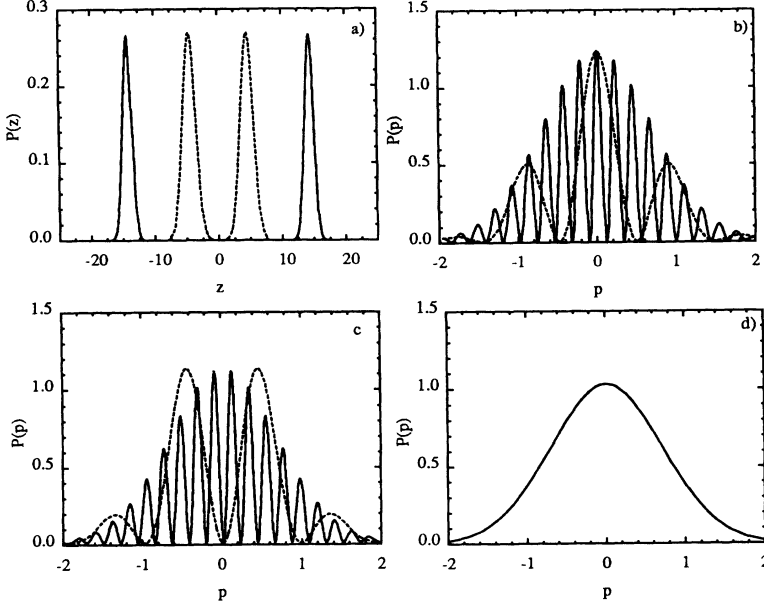


FIG. 1. Plots of the momentum probability distribution $P(p)$ and position probability distribution $P(z)$. (a) Plot of $P(z)$ versus z for the superposition state $|\varphi_+\rangle$. Here $g = 2.5$ and $\lambda/g^2 = 100$ for the solid line; $g = 2.5$ and $\lambda/g^2 = 5$ for the dotted line. (b) Plot of $P(p)$ versus p for the superposition state $|\varphi_+\rangle$. Here $g = 2.5$ and $\lambda/g^2 = 100$ for the solid line; $g = 2.5$ and $\lambda/g^2 = 5$ for the dotted line. (c) Plot of $P(p)$ versus p for the superposition state $|\varphi_-\rangle$. Here $g = 2.5$ and $\lambda/g^2 = 100$ for the solid line; $g = 2.5$ and $\lambda/g^2 = 5$ for the dotted line. (d) Plot of $P(p)$ versus p for the steady-state intracavity field of the parametric oscillator state (3.3) with $g = 2.5$ and $\lambda/g^2 = 100$. The same result is obtained for a 50-50 mixture of the superposition states $|\varphi_+\rangle$ and $|\varphi_-\rangle$.

$$H = -i\hbar \left[\frac{\bar{g}^* \epsilon^*}{2\gamma_2} a_1^2 - \frac{\bar{g}\epsilon}{2\gamma_2} a_1^{\dagger 2} \right] + a_1^2 \Gamma^\dagger + a_1^{\dagger 2} \Gamma. \quad (3.6)$$

One has a two-photon pumping and a two-photon loss (here Γ and Γ^\dagger represent reservoirs), brought about by the parametric interaction. It is seen that the signal, which is coupled only to the pump via the down-conversion process, can absorb or emit photons only in pairs. Thus, in the absence of cavity loss, if the signal is initially in a vacuum state it can evolve only to the coherent superposition $|\varphi_+\rangle$, which has an even photon number. The time needed for this evolution will be determined by the strength of the two-photon nonlinearity. The loss of signal photons from the cavity through the end mirrors allows the formation of the odd photon number state. The final steady state formed over a number of cavity lifetimes is thus the mixture of the two superposition states. It might be expected, however, that “something close to” the macroscopic superposition state $|\varphi_+\rangle$ is generated in a transient regime. This is provided the signal cavity lifetime is sufficiently long, which corresponds to the regime of sufficiently large g .

We now ask whether Schrödinger-cat states exhibiting any quantum interference fringes do in fact exist on time scales smaller than the cavity relaxation time and for finite values of g . To answer this it becomes necessary to solve for the evolution of the oscillator.

IV. SIMULATION OF THE STOCHASTIC EQUATIONS

In this section we present results obtained from the numerical simulation of the stochastic equations. We evaluate the quadrature phase amplitude probability distribution functions $P(z)$ and $P(p)$, defined in the preced-

ing section. These probability distributions are obtained from the positive P function as

$$P(z) = \langle z|\rho|z\rangle = \int P(\alpha_1, \alpha_1^\dagger) \frac{\langle z|\alpha_1\rangle \langle \alpha_1^\dagger|z\rangle}{\langle \alpha_1^\dagger|\alpha_1\rangle} d^2\alpha_1 d^2\alpha_1^\dagger. \quad (4.1)$$

Similarly

$$P(p) = \langle p|\rho|p\rangle = \int P(\alpha_1, \alpha_1^\dagger) \frac{\langle p|\alpha_1\rangle \langle \alpha_1^\dagger|p\rangle}{\langle \alpha_1^\dagger|\alpha_1\rangle} d^2\alpha_1 d^2\alpha_1^\dagger. \quad (4.2)$$

We have used the following coordinate and momentum representation results for the coherent state:

$$\langle z|\alpha_1\rangle = \pi^{-1/4} \exp\left\{-\frac{z^2}{2} + \sqrt{2}z\alpha_1 - \frac{\alpha_1^2}{2} - \frac{|\alpha_1|^2}{2}\right\}, \quad (4.3)$$

$$\langle p|\alpha_1\rangle = \pi^{-1/4} \exp\left\{-\frac{p^2}{2} - i\sqrt{2}p\alpha_1 + \frac{\alpha_1^2}{2} - \frac{|\alpha_1|^2}{2}\right\}. \quad (4.4)$$

Here $|z\rangle$ and $|p\rangle$ are position and momentum eigenstates, respectively. One may evaluate $P(z)$ and $P(p)$ by averaging over all trajectories the quantities $\langle z|\alpha_1\rangle \langle \alpha_1^\dagger|z\rangle / \langle \alpha_1^\dagger|\alpha_1\rangle$ and $\langle p|\alpha_1\rangle \langle \alpha_1^\dagger|p\rangle / \langle \alpha_1^\dagger|\alpha_1\rangle$, respectively.

The numerical simulations of the stochastic equations were performed using the weak semi-implicit method of integration, the stochastic equations being first rewritten to include Stratonovich correction terms. The relative merits of this integration technique have been discussed

in depth by Drummond and Mortimer [22]. A boundary condition was incorporated into the numerical algorithm to ensure that trajectories did not escape the manifold. Because the size of the noise terms scaled as g , large ensemble sizes were required to obtain convergence for the larger g values. In order to estimate the sampling error associated with the finite limitation of ensemble sizes, a calculation was performed with n subensembles of N trajectories each. This enabled error bounds to be placed on averages calculated [10].

V. NUMBER STATE CALCULATIONS

An alternative method for obtaining the transient solutions of the degenerate parametric oscillator is to solve the master equation directly in a number state basis. For systems where the mean photon number is not too large, the number state method provides another technique for solving the nonlinear system. Let us expand the density matrix in the number state basis as

$$\rho_{nm} = \langle n|\rho|m\rangle \quad (5.1)$$

The signal field of the degenerate parametric oscillator in the limit where the pump is adiabatically eliminated is described by the master equation

$$\begin{aligned} \frac{d\rho}{d\tau} = & \frac{\lambda}{2} \left[a_1^{\dagger 2} - a_1^2, \rho \right] \\ & + \frac{g^2}{2} \left[2a_1^2 \rho a_1^{\dagger 2} - a_1^{\dagger 2} a_1^2 \rho - \rho a_1^{\dagger 2} a_1^2 \right] \\ & + \left[2a_1 \rho a_1^{\dagger} - a_1^{\dagger} a_1 \rho - \rho a_1^{\dagger} a_1 \right]. \end{aligned} \quad (5.2)$$

Here the last term in square brackets (proportional to γ_1 in real time) represents the signal cavity loss. The remaining terms proportional to λ and g^2 are the two-photon pump and two-photon loss terms, respectively, resulting from the coupling via the parametric nonlinearity to the adiabatically eliminated pump cavity mode. The validity of this master equation has been investigated rigorously by Mortimer and Risken [23], and the correspondence to the stochastic equations (2.4) may be established by expanding (5.2) in terms of the positive P representation using standard procedures. The two-photon loss and pump terms associated with the above master equation are derivable from the model Hamiltonian (3.6). Now expanding over the number state basis we may express the time evolution of the system as

$$\frac{\partial}{\partial \tau} \rho_{nm} = \left\langle n \left| \frac{\partial}{\partial \tau} \rho \right| m \right\rangle = \mathcal{L}_{ij}^{nm} \rho_{nm}, \quad (5.3)$$

where this supermatrix \mathcal{L}_{ij}^{nm} is given by

$$\begin{aligned} \mathcal{L}_{ij}^{nm} = & \frac{\lambda}{2} \sqrt{i(i-1)} \delta_{i,j}^{n+2,m} + \frac{\lambda}{2} \sqrt{j(j-1)} \delta_{i,j}^{n,m+2} - \frac{\lambda}{2} \sqrt{(i+1)(i+2)} \delta_{i,j}^{n-2,m} - \frac{\lambda}{2} \sqrt{(j+1)(j+2)} \delta_{i,j}^{n,m-2} \\ & - [i+j] \delta_{i,j}^{n,m} + 2\sqrt{(i+1)(j+1)} \delta_{i,j}^{n-1,m-1} - g^2 [i(i-1) + j(j-1)] \delta_{i,j}^{n,m} \\ & + 2\sqrt{(i+1)(i+2)(j+1)(j+2)} \delta_{i,j}^{n-2,m-2}. \end{aligned} \quad (5.4)$$

Here the Dirac δ function is

$$\delta_{i,j}^{n,m} = \begin{cases} 1 & \text{if } i = n, \quad j = m \\ 0 & \text{otherwise.} \end{cases} \quad (5.5)$$

Rigorously, the master equation corresponds to a matrix of infinite order. Technically, to allow numerical approximations, one must establish a finite cutoff by putting a finite limit on the number of number states used in the basis. Such a procedure is practical for systems of small or moderate photon number. The number of number states needed as a basis is chosen so that the effect of increasing the number of states is insignificant. We need to determine the probability distribution functions $P(p)$ and $P(z)$ in order to establish evidence for a superposition state. We may write

$$P(z) = \langle z|\rho|z\rangle, \quad (5.6)$$

$$P(p) = \langle p|\rho|p\rangle, \quad (5.7)$$

which can be written in terms of the density matrix element ρ_{nm} (obtained by solution of the master equation in the number state basis) as

$$P(z) = \sum_n \sum_m \langle z|n\rangle \rho_{nm} \langle m|z\rangle, \quad (5.8)$$

$$P(p) = \sum_n \sum_m \langle p|n\rangle \rho_{nm} \langle m|p\rangle. \quad (5.9)$$

In Eqs. (5.8) and (5.9), $\langle z|n\rangle$ and $\langle p|n\rangle$ are given by

$$\langle z|n\rangle = (2^n n!)^{-\frac{1}{2}} \left(\frac{\eta}{\pi} \right)^{\frac{1}{4}} \exp \left[-\frac{1}{2} \eta z^2 \right] H_n(z\sqrt{\eta}), \quad (5.10)$$

$$\langle p|n\rangle = (2^n n!)^{\frac{1}{2}} (-i)^n \left(\frac{\hbar^2}{\pi\eta} \right)^{\frac{1}{4}} \exp \left[-\frac{1}{2} \frac{\hbar^2 p^2}{\eta} \right] H_n \left(\frac{\hbar p}{\sqrt{\eta}} \right), \quad (5.11)$$

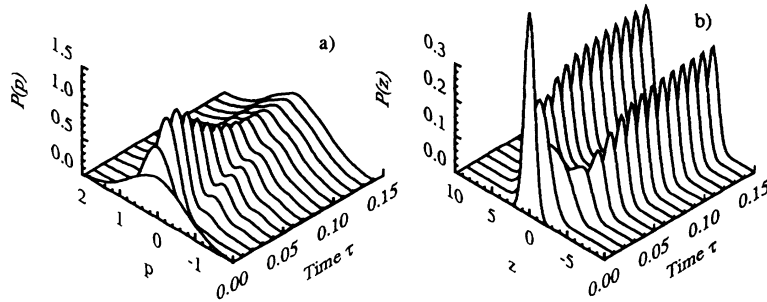


FIG. 2. Plot of the evolution of (a) the momentum probability distribution $P(p)$ and (b) the position probability distribution $P(z)$. Here $g = 2.5$ with $\lambda/g^2 = 10$ and τ is the cavity decay time for the signal mode.

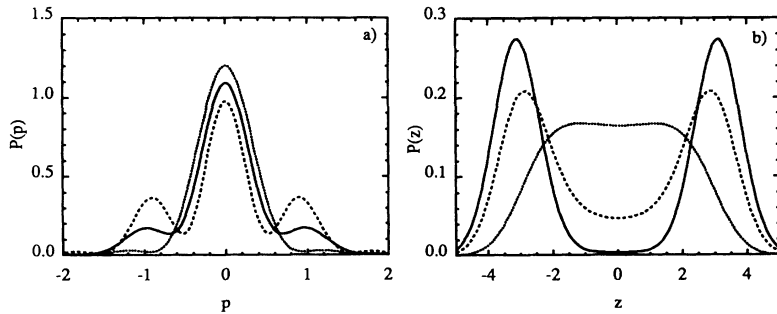


FIG. 3. Plot of (a) the momentum probability distribution $P(p)$ and (b) the position probability distribution $P(z)$ for the stochastic simulations at times $t = 0.0025\tau$ (dotted), $t = 0.0050\tau$ (dashed), and $t = 0.0100\tau$ (solid). Here $g = 10.0$ and $\lambda/g^2 = 5$.

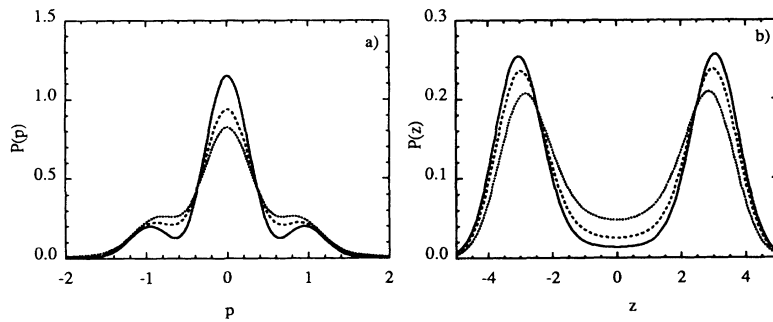


FIG. 4. Plot of (a) the momentum probability distribution $P(p)$ and (b) the position probability distribution $P(z)$ for the stochastic simulations at times $t = 0.015\tau$ (dotted), $t = 0.020\tau$ (dashed), $t = 0.025\tau$ (solid). Here $g = 5.0$ and $\lambda/g^2 = 5$.

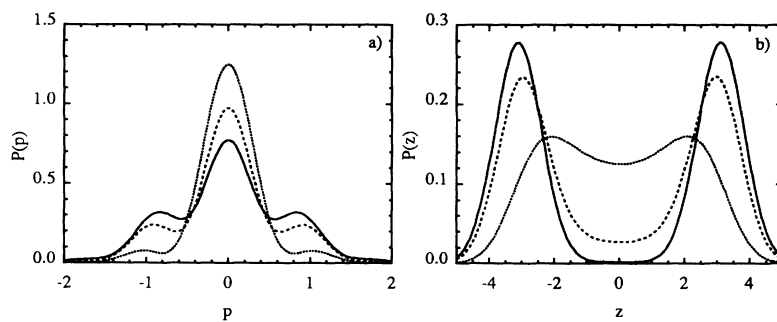


FIG. 5. Plot of (a) the momentum probability distribution $P(p)$ and (b) the position probability distribution $P(z)$ for the stochastic simulations at times $t = 0.050\tau$ (dotted), $t = 0.100\tau$ (solid), and $t = 0.200\tau$ (dashed). Here $g = 2.5$ and $\lambda/g^2 = 5$.

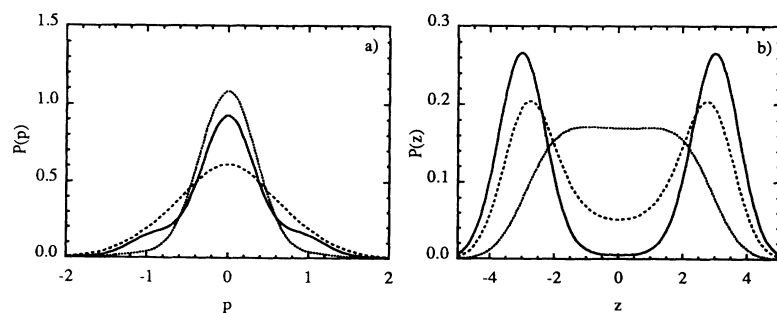


FIG. 6. Plot of (a) the momentum probability distribution $P(p)$ and (b) the position probability distribution $P(z)$ for the stochastic simulations at times $t = 0.125\tau$ (dotted), $t = 0.250\tau$ (solid), $t = 0.500\tau$ (dashed). Here $g = 1.45$ and $\lambda/g^2 = 5$.

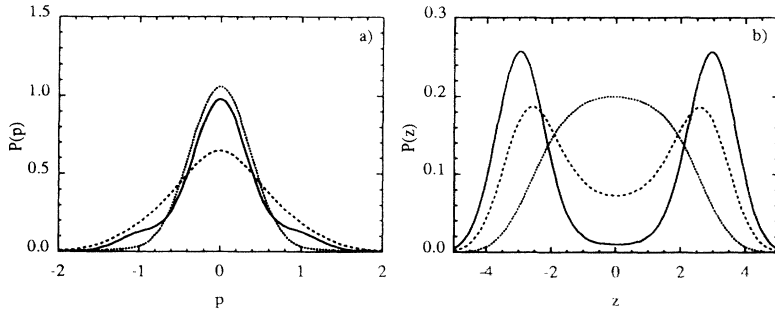


FIG. 7. Plot of (a) the momentum probability distribution $P(p)$ and (b) the position probability distribution $P(z)$ for the stochastic simulations at times $t = 0.125\tau$ (dotted), $t = 0.250\tau$ (solid), and $t = 0.500\tau$ (dashed). Here $g = 1.35$ and $\lambda/g^2 = 5$.

where $\eta = \sqrt{\frac{k\eta m}{\hbar}}$ and $H_n(z)$ is the Hermite polynomial. Hence once our master equation has been solved numerically in the number state basis to give $\rho_{n,m}$, one can easily determine the probability distribution functions $P(p)$ and $P(z)$.

VI. DISCUSSION OF RESULTS

For a comparison with the oscillator results, we first examine (Fig. 1) the quadrature phase amplitude distributions $P(z)$ and $P(p)$ for the (ideal) quantum superposition state $|\varphi_+\rangle$. The plots for the ideal state $|\varphi_-\rangle$ are similar, except for a shifting of the positions of the interference maxima and minima which occurs in the $P(p)$ distribution. Figure 1(d) shows the momentum probability distribution $P(p)$ calculated for a 50-50 classical mixture of $|\varphi_+\rangle$ and $|\varphi_-\rangle$. In this case, no fringes are observed. Also shown is the distribution for the steady-state mixture given by (3.3), for $\lambda/g^2 = 100$.

The results obtained for $P(z)$ and $P(p)$ upon simulations of the stochastic equation (2.4) are shown in Figs. 2–7. These represent the predictions for the signal field of the degenerate parametric oscillator in the adiabatic

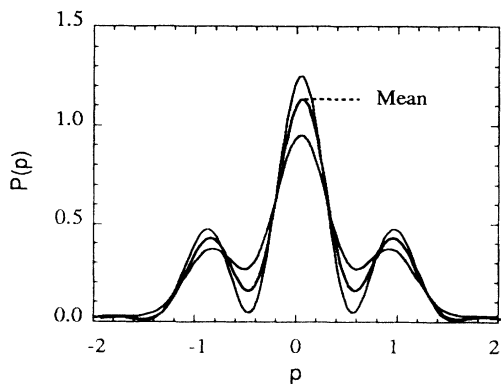


FIG. 8. Plot of the error estimate for the momentum probability distribution $P(p)$. Here $g = 2.5$ and $\lambda/g^2 = 5$. The time has been set to $t = 0.1\tau$. The thick curve corresponds to the mean of 10 subensembles of 100 000 runs. The thin curves correspond to the standard error in this mean.

limit with $\gamma_2 \gg \gamma_1$, where the signal is initially in a vacuum state. As predicted from analytical calculations [17], the steady-state or long-time distributions for the parametric oscillator reveal no interference fringes. The formation of fringes with the evolution of the signal field from the vacuum state is clearly evident in Fig. 2, where $g = 2.5$ and $\lambda/g^2 = 10$. The first minimum appearing at approximately $p = \pi g/\sqrt{8\lambda}$ is consistent with the formation of the state $|\varphi_+\rangle$. Also evident from Fig. 2 is the washing out of the interference pattern as the oscillator evolves further. The $|\varphi_-\rangle$ state, which is generated from $|\varphi_+\rangle$ with the loss of a cavity photon, contributes more significantly as time increases, and the fringes are lost in this case after only 0.1τ . The long-time distribution compares well with the probability distribution [Fig. 1(d)] for the steady-state solution (3.3) predicted analytically for the large g limit.

In order to establish the orders of g required to obtain a clear fringe pattern, the $P(z)$ and $P(p)$ distributions are shown in Figs. 3–7 for a range of g and for fixed $\lambda/g^2 = 5$. For g greater than or of the order of 1.45, interference fringes become clearly apparent in the transient evolution of the oscillator. The fringes (for fixed λ/g^2) become more pronounced as g increases. This is consistent with the earlier analytical conclusions, which were based on calculations performed in the large g limit where the strength of the two-photon nonlinearity is much greater than the single-photon cavity loss rate. The results of the simulations indicate the appearance of quite visible fringes for $g \sim 5$. Figure 8 shows typical error bounds for the simulation method for $g = 2.5$ and $\lambda/g^2 = 5$. All results here have, however, also been obtained using number state expansion of the master equation.

The plots in Figs. 3–7 are for relatively low photon number determined here by the magnitude of λ/g^2 . The analytical results of Wolinsky and Carmichael indicate $|\varphi_+\rangle$ formed at arbitrary λ/g^2 for sufficiently large g . In order to answer the question of what values of g are required to obtain superposition effects for higher λ/g^2 , we present in Fig. 9 results of an extensive numerical calculation where $g = 2.5$ and $\lambda/g^2 = 100$. The larger λ/g^2 value represents a larger separation in phase space of the two coherent states and hence is closer to a “true Schrödinger cat.” We observe clear evidence of the formation of $|\varphi_+\rangle$, even for the relatively low g value of $g = 2.5$. A similar fringe pattern is obtained if one considers an 80-20 classical mixture of the $|\varphi_+\rangle$ and $|\varphi_-\rangle$ states.

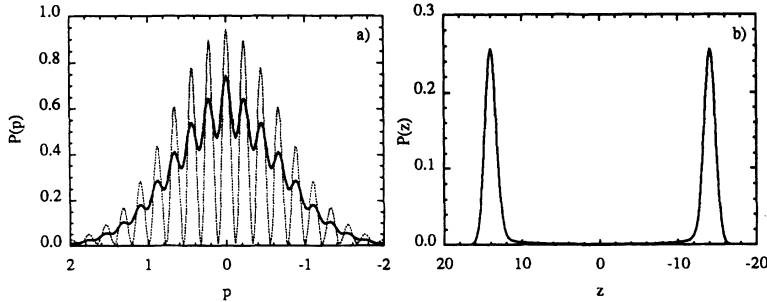


FIG. 9. Plot of (a) the momentum probability distribution $P(p)$ and (b) the position probability distribution $P(z)$. These calculations are plotted for $g = 2.5$, $\lambda/g^2 = 100$, and $t = 0.01\tau$. We have also plotted (dotted line) in (a) the pure superposition state $|\varphi_+\rangle$.

VII. CONCLUSION

We have obtained numerical predictions for the evolution from a vacuum state of the intracavity signal mode of the degenerate parametric oscillator. The solutions are obtained in the adiabatic limit where the decay of the pump cavity mode is much greater than that of the signal. Above the semiclassical threshold, and for sufficiently large λ/g^2 , the probability distribution for one of the quadrature phase amplitudes (z say) becomes clearly bimodal. For sufficiently large g ($g > 1$), the corresponding probability distribution for the orthogonal quadrature phase amplitude (p say) develops transient interference fringes. The experimental observation of such fringes would be evidence for the formation of a quantum superposition of two coherent states well separated in phase space. Such states, for very large λ/g^2 values, are analogous to the ‘‘Schrödinger-cat’’ states discussed by Schrödinger in his famous paradox. Our results have been limited for practical numerical reasons to values for λ/g^2 of the order 100. Nevertheless the observation of such superpositions of mesoscopically distinct states

would be a significant advance.

The analysis given by Carmichael and Wolinsky of systems with arbitrarily large λ/g^2 applies only to the large g limit. Our complete solutions indicate that values of $g \sim 2.5$ will give clear interference fringes for $\lambda/g^2 \sim 100$. In this case the probability distribution for the quadrature phase amplitude z is clearly bimodal with minimal overlap between the two peaks. Typical optical degenerate parametric oscillators to date have very small g values, at least several orders of magnitude smaller than those considered here. The nonlinearity to cavity loss ratio is thus much too small to anticipate observation of the fringes discussed here. Nevertheless our work showing clear fringes to be predicted for g values not much greater than 1 is encouraging. Systems obtaining values of g of this order would not seem out of the question. Such values may be obtainable using Josephson nonlinearities [11]. While the distinction in phase space between the two states associated with z must (for $\lambda/g^2 = 100$) be considered mesoscopic, the observation of such fringes would be a first step towards the observation of true Schrödinger-cat states, where the two states of z are macroscopically separated.

- [1] L. Wu, H.J. Kimble, J.L. Hall, and H. Wu, *Phys. Lett.* **57**, 2520 (1986).
- [2] A. Heidmann, R.J. Horowicz, S. Reynaud, E. Giacobino, C. Fabre, and G. Camy, *Phys. Rev. Lett.* **59**, 2555 (1987).
- [3] Z.Y. Ou, S.F. Pereira, H.J. Kimble, and K.C. Peng, *Phys. Rev. Lett.* **68**, 3663 (1992).
- [4] R. Graham, in *Quantum Statistics in Optics and Solid-State Physics*, edited by G. Hohler, Springer Tracts in Modern Physics Vol. 66 (Springer, New York, 1973), p. 1; *Phys. Lett. A* **32**, 373 (1970); R. Graham and H. Haken, *Z. Phys.* **210**, 319 (1968).
- [5] P.D. Drummond, K.J. McNeil, and D.F. Walls, *Opt. Acta* **28**, 211 (1981).
- [6] B. Yurke, *Phys. Rev. A* **29**, 408 (1984).
- [7] M.J. Collett and C.W. Gardiner, *Phys. Rev. A* **30**, 1386 (1984); M.J. Collett and D.F. Walls, *ibid.* **32**, 2887 (1985).
- [8] M.D. Reid and P.D. Drummond, *Phys. Rev. Lett.* **60**, 2731 (1988); P.D. Drummond and M.D. Reid, *Phys. Rev. A* **41**, 3930 (1990).
- [9] S. Reynaud, C. Fabre, and E. Giacobino, *J. Opt. Soc. Am. B* **4**, 1520 (1987).
- [10] P. Kinsler and P.D. Drummond, *Phys. Rev. Lett.* **64**, 236 (1989); P.D. Drummond and P. Kinsler, *Phys. Rev. A* **40**, 4813 (1989).
- [11] B. Yurke, P.G. Kaminsky, R.E. Miller, E.A. Whittaker, A.D. Smith, A.H. Silver, and R.W. Simon, *Phys. Rev. Lett.* **60**, 764 (1988).
- [12] M. Wolinsky and H.J. Carmichael, *Phys. Rev. Lett.* **60**, 1836 (1988); M. Wolinsky, Ph.D. thesis, The University of Texas, Austin, 1990.
- [13] H.J. Carmichael and M. Wolinsky, *OSA Annual Meeting, 1989 Technical Digest Series Vol. 18* (Optical Society of America, Washington, DC, 1989).
- [14] E. Schrödinger, *Naturewissenschaften* **23**, 812 (1935).
- [15] B. Yurke and D. Stoler, *Phys. Rev. Lett.* **57**, 13 (1986).
- [16] A.J. Leggett, in *Directions in Condensed Matter Physics*, edited by G. Grinstein and G. Mazenko (World Scientific, Singapore, 1985); in *Proceedings of the International Symposium on Foundations of Quantum Mechanics*, edited by S. Kamefuchi *et al.* (Physical Society of Japan, Tokyo, 1983); A.O. Calderia and A.J. Leggett, *Phys. Rev. A* **31**, 1059 (1985); A. Leggett and C. Garg, *Phys. Rev. Lett.* **54**, 857 (1985); A. Mecozzi and P. Tombesi, *ibid.* **58**, 1055 (1987); G.J. Milburn and C.A. Holmes, *ibid.* **56**, 2237 (1986); S. Song, B. Yurke, and C.M. Caves, *Phys. Rev. A* **41**, 5261 (1990); T.A.B. Kennedy and D.F. Walls, *ibid.* **37**, 152 (1988); H.J. Carmichael, L. Tian, W. Ren, and P. Alsing, in *Cavity Quantum Electrodynamics*, edited by P. Berman (Aca-

- demic Press, Boston, 1994); H.J. Carmichael, P. Kochan, and L. Tian, in *Proceedings of the International Symposium on Coherent States: Past, Present, and Future, Oak Ridge, Tennessee, 1993*, edited by D.H. Feng, J. R. Klauder, and M. R. Strayer (World Scientific, Singapore, 1993), p. 75; M.D. Reid and L. Krippner, *Phys. Rev. A* **47**, 552 (1992); M. Kitagawa and Y. Yamamoto, *ibid.* **34**, 3974 (1986); G.J. Milburn, *ibid.* **33**, 674 (1986); T.A.B. Kennedy and P.D. Drummond, *ibid.* **38**, 1319 (1988); C.M. Savage and W.A. Cheng, *Opt. Commun.* **70**, 439 (1989); B.C. Sanders, *Phys. Rev. A* **44**, 5913 (1989); P. Meystre, J. Slosser, and M. Wilkens, *ibid.* **43**, 6458 (1991); B. Yurke, W. Schleich, and D.F. Walls, *ibid.* **42**, 5261 (1990); A. La Porta, R.E. Slusher, and B. Yurke, *Phys. Rev. Lett.* **62**, 26 (1989); B. Yurke, *J. Opt. Soc. Am. B* **2**, 732 (1986); H.J. Carmichael, J.S. Satchael, and S. Sarkar, *Phys. Rev. A* **34**, 3166 (1986).
- [17] M.D. Reid and B. Yurke, *Phys. Rev. A* **46**, 4131 (1992).
[18] P.D. Drummond and C.W. Gardiner, *J. Phys A* **13**, 2353 (1980).
[19] R. Schack and A. Schenzle, *Phys. Rev. A* **43**, 6303 (1990).
[20] A.M. Smith and C.W. Gardiner, *Phys. Rev. A* **39**, 3511 (1989).
[21] C.W. Gardiner (unpublished).
[22] P.D. Drummond and I.K. Mortimer, *J. Comput. Phys.* **93**, 144 (1991).
[23] I.K. Mortimer and H. Risken, *Phys. Rev. A* **44**, 617 (1991).